Filtered particle tracking in isotropic turbulence and stochastic modeling of subgrid-scale dispersion

By Jacek Pozorski † AND Sourabh V. Apte ‡

A numerical study based on the Eulerian-Lagrangian formulation is performed for dispersed phase motion in a turbulent flow. The effect of spatial filtering, commonly employed in large-eddy simulations, and the role of the subgrid scale turbulence on the statistics of heavy particles, including preferential concentration, are studied through *a priori* analysis of DNS of particle-laden forced isotropic turbulence. A stochastic Langevin model is proposed to reconstruct the residual (or subgrid scale) fluid velocity along particle trajectories. In simulations where the subgrid scale kinetic energy attains 30–35% of the total we observe the impact of residual fluid motions on particles of a smaller inertia. It is shown that neglecting the influence of subgrid scale fluctuations has a significant effect on the preferential concentration of those particles. The computation results for a selection of particle inertia parameters are performed to appraise the model through comparisons of particle turbulent kinetic energy and the statistics of preferential concentrations.

1. Introduction

Numerical studies of two-phase flows with dispersed droplets or solid particles constitute an important activity in turbulence research. Both in the two-fluid and the trajectory approach (e.g., Simonin 1996, Minier & Peirano 2001) there remain a variety of open theoretical and modeling issues. Practical applications of two-phase polydispersed flows include environmental studies, chemical and process engineering, as well as power engineering, including wet steam flows and combustion of solid or liquid fossil fuels. A relevant industrial example is fuel injection in Diesel engine or a gas turbine combustor where the dispersed phase is present in the form of small droplets (Apte *et al.* 2003, Moin & Apte 2006).

Historically, the trajectory approach with random walk ideas dates back to the landmark paper of Taylor (1921). Since then, the Lagrangian stochastic approach has been developed in its natural context for modeling and prediction of turbulent diffusion and dispersion. In the framework of statistical RANS (Reynolds-averaged Navier-Stokes) description of turbulence, various random walk models for the diffusion of fluid particles (Thomson 1986, Sawford 2001) and the dispersion of solid particles in two-phase flows have been proposed, cf. Stock (1996), Pozorski & Minier (1998) and references therein. Moreover, a general probability density function (PDF) formalism has been developed (Reeks 1992, Pozorski & Minier 1999, Minier & Peirano 2001, Mashayek & Pandya 2003, Peirano *et al.* 2006). A review and some discussion of these issues is given in Sec. 2.2.

Nowadays, following a rapid progress in large eddy simulation (LES) of turbulence,

† Institute of Fluid-Flow Machinery, Polish Academy of Sciences, Gdańsk, Poland
‡ Oregon State University, USA

the LES method has been used with success to compute two-phase dispersed flows. In single-phase LES, the residual or subgrid-scale (SGS) flow scales remain unresolved by definition and their impact on the resolved motion is usually accounted for through an appropriate SGS stress model. In dispersed two-phase flows, the feasibility of LES to study preferential concentration of particles by turbulence (Wang & Squires 1996) and to compute flows with two-way momentum coupling (Boivin *et al.* 2000) has been reported. In the Lagrangian-Eulerian studies of dispersed flows (i.e., LES of the continuous phase coupled with particle tracking) it has been a common practice to neglect the SGS flow scales. It has been argued that the long-time particle dispersion is governed by the resolved, larger-scale fluid eddies (Armenio *et al.* 1999). Only recently, the influence of the SGS flow turbulence on the statistics of particle motion and their preferential concentration has received some attention in the literature.

Generally speaking, the main difficulty in extending LES to physically-complex flows, such as dispersed two-phase flows, comes from the fact that some terms in the filtered LES evolution equations have to be modeled altogether, because relevant physical processes occur at unresolved scales. An example are the source terms, due to chemical reactions, in mass and energy balance equations. Some other are partly resolved convective terms and source terms due to the presence of particles: mass transport (evaporation/condensation), momentum coupling, and energy balance (heating, latent heat of evaporation). It remains an open question to determine in what cases the SGS part of these terms should be accounted for when considering the behavior of the dispersed phase. In addition, new models for the subgrid scale effects on the particle motion are necessary to correctly predict particle dispersion in LES.

In the following, we first recall the issue of particle dispersion in the context of RANS and LES turbulence modeling (Sec. 2). The main emphasis of the paper is to revisit the role of the unresolved fluid turbulence in LES of particle-laden flows (also called SGS particle dispersion). This is done with the help of *a priori* LES tests using filtered DNS velocity fields, both without and with a model to account for the SGS turbulence "seen" by particles. This approach is referred to as the filtered particle tracking (FPT). The first aim is to study the impact of LES filtering on the particulate phase (Sec. 3). The effect will be shown to be non-negligible for a sufficiently coarse LES mesh (judged by a residual kinetic energy content). A quantitative assessment of this effect is accomplished through particle velocity statistics and the statistics of preferential particle concentration: the probability distribution of particle number density and the radial distribution function of the interparticle distance. The second aim of the paper is to develop a model for the SGS particle dispersion (Sec. 4). The model is meant to reconstruct statistically the residual flow field along particle trajectories. Computation results are reported (Sec. 5) for the forced isotropic turbulence case: turbulent kinetic energy of particles, particle velocity autocorrelation time scale, and measures of preferential concentration.

2. Turbulent dispersion of particles

2.1. *Problem statement*

In the paper, the dispersed phase will be assumed dilute; consequently, the one-way momentum coupling is adequate and particle collisions can safely be neglected. Yet, for a sufficiently high load of the dispersed phase, the two-way coupling needs to be accounted for in the momentum and energy equations; moreover, for high particle number densities, the interparticle collisions will affect their dynamics. Additional complexity to

the physical picture would be added through the interphase mass and energy transfer in the case of evaporating droplets or volatilizing solid particles. Here, we concentrate on the dynamical aspects only, and precisely on the impact of turbulence on the statistics of the dispersed phase.

To determine the evolution of a set of non-interacting solid particles in turbulent flow, particle location $\mathbf{x}_p$ and its velocity $\mathbf{U}_p$ should be known. Another variable of importance for further considerations is the fluid velocity $\mathbf{U}^*$ "seen" or sampled by the particle as it moves across the flow. In terms of the instantaneous Eulerian velocity field $\mathbf{U}(\mathbf{x}, t)$ of the carrier (fluid) phase, we have $\mathbf{U}^* = \mathbf{U}(\mathbf{x}_p, t)$. Respective governing equations for particles are:

$$\frac{d\mathbf{x}_p}{dt} = \mathbf{U}_p, \tag{2.1}$$

$$\frac{d\mathbf{U}_p}{dt} = \frac{3}{4}\frac{\rho_f}{\rho_p}\frac{C_D}{d_p}|\mathbf{U}^* - \mathbf{U}_p|(\mathbf{U}^* - \mathbf{U}_p)\ . \tag{2.2}$$

In general cases (Maxey & Riley 1983), the particle equation of motion (2.2) also includes the pressure-gradient, drag, added-mass and Basset forces. Yet, for particles much heavier than the carrier fluid, $\rho_p \gg \rho_f$ (ρ_f and ρ_p stand for fluid and particle densities, respectively), an acceptable approximation is often to retain only the aerodynamic drag and external force terms (if relevant). The drag coefficient, $C_D = C_D(\mathrm{R}_p)$, is a function of the particle Reynolds number, $\mathrm{R}_p = d_p|\mathbf{U}^* - \mathbf{U}_p|/\nu_f$ (based on the particle diameter d_p, the relative particle velocity, and the kinematic viscosity of the carrier fluid, ν_f). For the case of $\mathrm{R}_p \leq 1000$, the drag coefficient is approximated by a well-known correlation $C_D = (24/\mathrm{R}_p)(1 + 0.15\mathrm{R}_p^{0.687})$. In the limit of small R_p, the drag term takes the form $(\mathbf{U}^* - \mathbf{U}_p)/\tau_p$, written using the particle relaxation time $\tau_p = (\rho_p/\rho_f)d_p^2/18\nu_f$.

Obviously, modeling of the fluid velocities sampled by particles is no longer needed when the carrier phase is fully resolved, possibly with source terms that represent the exchange of mass, momentum, and energy between the particles and the flow. This is the DNS with point-particle tracking, Eqs. (2.1)–(2.2), where $\mathbf{U}^*$ is simply the instantaneous fluid velocity interpolated at the particle location. Since the number of degrees of freedom in turbulent flows scales as $\mathrm{R}^{9/4}$ with the Reynolds number R, this approach is feasible only for simple flow cases at relatively small R. Nevertheless, the DNS studies are extremely valuable for model testing, as evidenced in the following sections: preferential concentration patterns, first observed in experimental studies, are investigated (Sec. 3.3) and the impact of filtering on particle statistics is assessed (Sec. 3.4). For finite-size particles (of diameters comparable to the Kolmogorov scale η_K or larger), their dynamics, fluctuating lift and drag forces can be computed from "true DNS" studies (Bagchi & Balachandar 2003, Burton & Eaton 2003).

2.2. *Turbulent dispersion in RANS*

Despite the growing importance of DNS, a reduced (or contracted) description involving far less degrees of freedom is still used for practical, "real-life" flow cases. In particular, RANS remains a standard engineering approach. One of the difficult modeling aspects of turbulent dispersion in RANS is accounting for the fluid velocity statistics seen along the solid particle trajectories. They unavoidably differ from the "pure" Lagrangian statistics because of the particle inertia (related to the relaxation time τ_p of particle momentum) and the effect of external forces (such as gravity). Stochastic models based on the Langevin equation have been proposed to account for these effects (Pozorski & Minier 1998, Minier *et al.* 2004). Alternatively, the PDF formalism, initially developed in tur-

bulence modeling (cf. Pope 2000), and particularly useful in turbulent combustion (Fox 2003), has been extended to turbulent dispersion issues, starting with the kinetic equation of Reeks (1992) and further developed by Pozorski & Minier (1999). The system of flow variables consists of $\mathbf{x}_p$, $\mathbf{U}_p$, and $\mathbf{U}^*$. In the Lagrangian notation, particles are identified by their location $\mathbf{x}_p^0$ at a tagging time t^0, that is $\mathbf{x}_p(t^0;\mathbf{x}_p^0) = \mathbf{x}_p^0$; so are the velocities "seen" by particles: $\mathbf{U}^*(t;\mathbf{x}_p^0) = \mathbf{U}(\mathbf{x}_p(t;\mathbf{x}_p^0),t)$. Particle location and velocity are governed by Eqs. (2.1) and (2.2), whereas $\mathbf{U}^*$ evolves according to $d\mathbf{U}^*/dt = \mathbf{A}$ where the acceleration $\mathbf{A}$ of the fluid "seen" should be modeled. This can be done by the stochastic diffusion processes (the Langevin equation) with a proper account for gravity $\mathbf{g}$ and particle inertia. The kinetic equation of Reeks (1992) governs the transport of the joint PDF of $\mathbf{x}_p$ and $\mathbf{U}_p$ in a general case of nonhomogeneous turbulence. Actually, it is not the Fokker-Planck equation, since it is not local in time (history term is present); moreover, the diffusion matrix of the underlying stochastic process is not positive-definite (Minier & Pozorski 1997). An alternative derivation of the kinetic equation has been proposed (Pozorski 1998) based on the cumulant expansion technique. It has also been shown (Pozorski & Minier 1999) that the modeled joint PDF of $\mathbf{x}_p$, $\mathbf{U}_p$ and $\mathbf{U}^*$ is governed by the Fokker-Planck equation.

In general terms, a physically-sound reconstruction of instantaneous fluid velocity "seen" by the particles $\mathbf{U}^*$ has to be performed out of limited information available (such as the fluid mean velocity $\langle\mathbf{U}\rangle$ and the turbulent energy). A classical approach goes through the decomposition $\mathbf{U}^* = \langle\mathbf{U}\rangle + \mathbf{u}^*$ with the mean fluid velocity at the particle location, $\langle\mathbf{U}\rangle(\mathbf{x}_p,t)$, determined from the Eulerian RANS solver for the carrier phase. (We recall that the simplistic assumption $\mathbf{U}^* = \langle\mathbf{U}\rangle$ is fundamentally wrong since it will predict no turbulent dispersion.) Various stochastic models have been proposed to represent the fluctuating fluid velocity $\mathbf{u}^*$ sampled by particles. They often are extensions of fluid diffusion models, developed in environmental and atmospheric studies, but can suffer from spurious drifts if improperly devised (MacInnes & Bracco 1992). A sound alternative is provided by a stochastic model for $\mathbf{U}^*$ (Minier & Peirano 2001, Sec. 7.5.2).

In the context of RANS, there are no instantaneous flow structures resolved; consequently, there is no preferential concentration which, by definition, denotes correlation of particle locations with certain flow structures (Eaton & Fessler 1994). In RANS of non-homogeneous turbulence, spatial gradients of particle number density can develop (even for initially uniform particle distribution) because of the so-called turbophoresis effect. It consists in the net particle displacement in the direction of decreasing turbulence intensity (for $\rho_p > \rho_f$). Still remaining on the grounds of statistical description, we note that a model for $\mathbf{U}^*$ is needed only in one-point closures. For a two-point, two-time PDF description, the fluid velocity $\mathbf{U}_2$ at the particle location $\mathbf{x}_2$ at t_2, given the particle location $\mathbf{x}_1$ at t_1, is determined from the velocity $\mathbf{U}_1$ and the conditional probability $f(\mathbf{U}_2;\mathbf{x}_2,t_2|\mathbf{U}_1;\mathbf{x}_1,t_1)$, cf. Zaichik & Alipchenkov (2003).

2.3. *Turbulent dispersion in LES*

In LES, the resolved (large-scale) part of the instantaneous flow field, $\tilde{\mathbf{U}}$ say, can readily be interpolated to particle locations. The major issue is now to determine whether the remaining (residual or subgrid-scale) part of the flow velocity field can have a noticeable influence on the particulate phase. In most studies reported so far, this influence has been neglected and justified by a low residual energy content. A LES of particle-laden channel flow was performed by Wang & Squires (1996). Analysis of their data (Fig. 4 there) shows that the ratio of the SGS kinetic energy $k_{\rm sg}$ to $\tilde{U}^2$ remains small throughout the viscous sublayer (roughly 10%). Also, Armenio *et al.* (1999) computed channel flow with the one-

way momentum coupling. Particles were tracked in a fully-resolved (DNS) velocity field and in filtered fields with up to 20% of the turbulent kinetic energy unresolved depending on the filter size; however, there was no filtering in the wall-normal direction. They performed then a corresponding LES with the same filter width Δ_f. In all cases, the r.m.s. particle dispersion was found to be only slightly affected by the incomplete resolution. Indeed, the time scale of particle velocity autocorrelation increases with increasing filter size, the particle turbulent kinetic energy decreases, and the long-term SGS dispersion is the product of the two quantities (cf. Shotorban & Mashayek 2005). However, the relative dispersion (cloud dispersion) will be affected by filtering.

Okong'o & Bellan (2004) performed an *a priori* analysis of a dispersed two-phase flow in mixing layers. They distinguished four possibilities for the reconstruction of the fluid velocities "seen": an ideal model (velocity U_i from DNS data), baseline model (velocity $\tilde{U}_i$ from LES), random model (velocity reconstructed as $\tilde{U}_i + \sigma\xi_i$ where ξ_i are Gaussian random numbers) and deterministic model (including the local Laplacian of the resolved field, cf. also Kuerten & Vreman (2005) for de-filtering in non-homogeneous directions). Oefelein (cf. Segura *et al.* 2004) extended the eddy life-time and interaction-time model known in RANS and successfully applied to the LES of channel flow. Also Sankaran & Menon (2002) proposed a simple SGS dispersion model, yet its impact on final LES results has not been reported. Moreover, it is not quite clear whether the successive residual velocities were generated there as independent random values at every flow time step or at time intervals prescribed otherwise.

Recently, Kuerten & Vreman (2005), Shotorban & Mashayek (2005), and Kuerten (2006) studied the application of approximate deconvolution model (ADM) for particle-laden flows. The ADM is theoretically supported as the inverse of LES filtering. It is deterministic and results in a kind of structural SGS model, since it aims to reconstruct (or mimic) the whole SGS flow field. In practice, ADM is able to retrieve only the largest unresolved scales (of the order of the cut-off length) by multiple implicit filtering. For a coarse-scale LES, one cannot (by definition) reconstruct all SGS flow (cf. also discussion in Okong'o & Bellan, 2000). So, for a slightly-filtered DNS ($\Delta_f = 2\eta_K$, say), ADM is expected to work (Kuerten & Vreman 2005). Otherwise, ADM is helpful in cases where particles are most responsive to scales just below the cut-off (Kuerten 2006). Shotorban & Mashayek (2006) also proposed a stochastic model for SGS particles dispersion and applied it to decaying isotropic turbulence. There, additional complexity resulted from the growth of η_K in time since relatively less and less energy was filtered out. In the present authors' opinion, the problem with that stochastic model was that no crossing-trajectory effect was accounted for. Hence, the integral time scale of the fluid "seen" by larger-inertia particles, and consequently, also the r.m.s. particle dispersion were over-estimated. On the contrary, the results for smaller-inertia particles were in good agreement with the DNS reference data.

An often overlooked conceptual difficulty related to LES with stochastic SGS dispersion modeling, as opposed to particle dispersion in RANS, comes from the fact that the latter is formulated in terms of statistical averages, whereas the nature of the former is more complex. Indeed, random-walk (or stochastic particle) models in the context of RANS are meaningful in terms of the statistics over particles (e.g., time-averaged for steady flows), such as their kinetic energy, dispersion coefficient, etc. On the other hand, the large-eddy flow field (obtained with local spatial averaging) can be thought of as a perfectly deterministic, instantaneous solution. The marginally-resolved flow scales can be partly retrieved through deterministic structural-type models (such as ADM, cf.

Kuerten 2006) what makes a consistent approach. Otherwise, the subfilter-scale motions remain statistical in nature and it is reasonable to conceive stochastic models for them. However, although these are single-realisation approaches in practical implementation, a question remains whether instantaneous particle variables are already physically meaningful, or again (as in RANS) should they be somehow averaged first. This is actually done here by the computation of the particle turbulent energy or by taking two-point correlations to analyse spatial segregation patterns. Basically, the problem refers to any stochastic model applied with LES (be it for dispersed flow, combustion, etc.) since, by definition, stochastic modeling uses the underlying concept of the PDF (or FDF) and only the ensemble-averaged quantities are of interest. In a strongly unsteady and/or inhomogeneous turbulence the use of just single realisations to predict the system behavior may not be appropriate.

3. Preferential concentration of particles in turbulent flows

3.1. *Effect of turbulent structures on particles*

Instantaneous structures of the turbulent velocity field influence the motion of heavy particles (droplets), depending on their inertia. A convenient definition of the particle Stokes number in isotropic turbulence goes through the normalization with the Kolmogorov time scale: $\mathrm{St} = \tau_p/\tau_K$. Particles of $\mathrm{St} = \mathcal{O}(1)$ tend to correlate with certain eddy structures and this leads to the effect of preferential concentration, i.e. accumulation of particles in flow regions of low vorticity and high rate of strain (streams, convergence zones); cf. Eaton & Fessler (1994) for review. Studies reported in the literature include DNS of isotropic turbulence (Squires & Eaton 1991, Wang & Maxey 1993) as well as LES (Wang & Squires 1996).

The preferential concentration changes the physical picture of particulate flows in a number of ways: it affects the particle deposition on walls (Uijttewaal & Oliemans 1996); it leads to an increase of interparticle collision rates and, possibly, coalescence in a dense two-phase flow regime (Reade & Collins 2000); it influences the particle settling velocity in an external (gravity) field (Wang & Maxey 1993). For particles that move in the external force field, their final settling velocity in turbulent fluid can be considerably larger than that observed in a stagnant fluid, depending on St. This effect has been first noticed in a laminar cellular flow field (Maxey 1987) and in random turbulence simulations (Wang & Maxey 1993). Arguably, the same physical mechanisms will lead to the increase of stopping distance of spray injected in turbulent flow due to the interaction of particles and vortical structures, specially in a final (low velocity) stage of particle motion.

3.2. *Quantifying preferential concentration*

Various measures of preferential concentration have been established in the literature, cf. Hogan & Cuzzi (2001) for a comparative study and sensitivity tests with respect to the Reynolds number and bin size. Preferential concentration can be quantified by the PDF of particle number density based on bin counting, cf. Fig. 1(a). The distribution of particle number $n = N_{PC}$ per bin (or per cell), $f_B(n)$, will depend on St and on the bin size. For a random (uncorrelated) distribution of particles in the domain, the PDF is the discrete Poisson distribution, $f_P(n)$, with the parameter λ being the mean of the number density (exactly: the average number of particles per cell, $\langle N_{PC} \rangle$)

$$f_P(n) = \frac{e^{-\lambda}}{n!}\lambda^n \,, \qquad \lambda = \langle N_{PC} \rangle \,. \tag{3.1}$$

A natural measure of the non-uniform particle concentration is the deviation of the actual (measured) number density from the random one (Wang & Maxey 1993):

$$\tilde{D} = \sum_{n=1}^{\infty} \left[f_B(n) - f_P(n) \right]^2 \ . \tag{3.2}$$

Another measure of preferential concentration is (Fessler *et al.* 1994)

$$D = \frac{s - s_P}{\lambda} \tag{3.3}$$

where s is the standard deviation of the actual number of particles per bin, and $s_P = \lambda^{1/2}$ is the standard deviation of the corresponding Poisson distribution; normally, $D \geq 0$.

Yet another possibility to quantify the non-uniform particle concentration comes from the two-point spatial distribution function. For a statistically isotropic and homogeneous system of particles, Reade & Collins (2000) introduced the radial distribution function (RDF) of the interparticle distance, $g(r)$, where $r = |\mathbf{x}_2 - \mathbf{x}_1|$ for particles located at points $\mathbf{x}_2$ and $\mathbf{x}_1$, cf. Fig. 1(b). The RDF is derived from the two-particle distribution function $g^{(2)}(\mathbf{x}_1, \mathbf{x}_2)$ under the assumption of isotropy. Basically, $g(r)dr$ is the number of particles located in a spherical cell $(r, r+dr)$ around $\mathbf{x}_1$, divided by the expected number of particles if their distribution were uniform, and averaged over first-particle locations $\mathbf{x}_1$. The RDF is close to unity for a uniformly distributed particle system. Moreover, $g(r)$ can provide a clear estimation of the characteristic length scale of preferential concentration (if any).

3.3. *DNS of particle-laden, forced isotropic turbulence*

The DNS of forced isotropic turbulence at $\mathrm{R}_\lambda \approx 40$ has been preformed on a 96^3 grid with periodic boundary conditions. A statistically stationary flow field was generated using a technique proposed by Lundgren (2003). Accordingly, a linear forcing function is added as a source term in the momentum equations. Starting from an initially random perturbation, the balance between the forcing function and viscous dissipation develops a stationary isotropic turbulent flow. The time step of the flow simulation was $\Delta t^+ = 3 \cdot 10^{-3}$. The particle tracking has been performed in the DNS velocity field (with the assumption of one-way momentum coupling) for a selection of St. In all simulations, we have used $64^3 = 262\,144$ particles which is deemed sufficient to keep the statistical error level reasonably low. The resulting snapshots of particle locations in a slice of the computational box are shown in Fig. 2. As readily noticed, the preferential concentration of particles is most visible for $0.2 < \mathrm{St} < 2$, in agreement with earlier observations of Squires & Eaton (1991).

The bin counting has been applied to particle locations in 3D with the bin size varying from the single cell size of the DNS ($\Delta_{\mathrm{bin}} = \Delta_f$) up to 1/6 of the domain size ($\Delta_{\mathrm{bin}} = 16\Delta_f$). As evidenced by the profiles of f_B in Fig. 3, the random particle pattern (the Poisson distribution) is noticed for the smallest particles tracked ($\mathrm{St} = 0.01$) for all bin sizes. Also for the largest particles ($\mathrm{St} = 4$) the pattern is basically random, specially for smaller bin sizes. Intermediate-size particles tend to deviate most from the random distribution. As noticed from Fig. 3(d), the limit behavior for large $\langle N_{PC} \rangle$ (larger bins) is well reproduced, i.e. the Poisson distribution, Eq. (3.1), tends to the Gaussian PDF, $\mathcal{N}(\lambda, \lambda^{1/2})$.

For particles in isotropic turbulence, $\tilde{D}$ computed from Eq. (3.2) is shown in Fig. 4(a);

the profile of D, Eq. (3.3), is shown in Fig. 4(b). Both confirm the visual impression from Fig. 2 that the maximum of preferential concentration occurs for particles of $\mathrm{St} = \mathcal{O}(1)$.

To better illustrate how the RDF $g(r)$ works in practice, we started with three simple, predetermined particle patterns in 3D (Fig. 5): uniform (particles distributed randomly), regularly ordered at some scale L (resulting in a checkered pattern), and ordered with some randomization. In the latter, particles were uniformly distributed in alternate boxes whose sizes were provided by the random numbers taken from the uniform distribution on intervals $(0.5L, 1.5L)$ in each coordinate direction. As quantified by the RDF in Fig. 6(a), the uniform random pattern from Fig. 5(a) does not exhibit any preferential concentration when looked at the scale of discretised RDF bins, Δr. The same remains true for any pattern (even perfectly regular) ordered at a short scale $l \ll \Delta r$. For the regular checkered pattern ($L > \Delta r$) from Fig. 5(b), the non-uniformities are clearly reflected in the RDF. It deviates from 1 to larger values when the preferential concentration occurs at a given separation. On the other hand, by definition of the RDF, it can drop to values smaller than 1 when at a given separation there are less particle pairs than for a uniform distribution. Moreover, the characteristic length scale of the pattern ($\sim L$) is retrieved from the plot (solid) in Fig. 6(a). When it comes to less regular particle arrangements (like the checkered, randomized pattern of Fig. 5c), the RDF plot becomes flatter. This is specially evident for the three-dimensional (3D) treatments. On the other hand, the RDF computed in 2D, when particles are located in a thin slice that represents a cut of the whole (3D) domain, seems to better visualise the segregation in "randomized" cases. For the checkered randomized pattern, the difference in the behaviour of the PDF (specially for larger r) is clearly noticed in Fig. 6(b). Accordingly, we have done some RDF computations of the heavy particle patterns in turbulent flow also in 2D (out of slices rather than boxes). The quite spectacular shape of the RDF for the pre-arranged patterns of Fig. 5(b,c) resembles that of the macroscopic density computed out of molecules' masses and locations (which is a well-known story when one discusses the shift from the atomic-scale to continuum limit for a liquid, say).

Then, we applied the RDF procedure in 3D to snapshots of particles moving in the DNS flow field. The plots in Fig. 7(a) show a departure from the uniform (random) distribution of particle locations in space, most pronounced for $0.2 < \mathrm{St} < 2$. The characteristic length scale of the pattern is about $10\eta_K$, again in line with the findings of Eaton & Fessler (1994). We note that the interpretation of the RDF plots is fairly subtle since the actual results depend on the choice of the RDF bin size Δr with respect to the scales (L or η_K) considered.

3.4. *A priori tests of preferential concentration: particle tracking in filtered DNS field*

To the best of the authors' knowledge, apart from the present study the effect of LES filtering on preferential particle concentration has been investigated only in a comprehensive paper by Fede & Simonin (2006). In the following, we report interesting findings from an *a priori* test. The instantaneous velocity field computed from DNS is subjected to spatial filtering to obtain the large-eddy velocity field. The filtering procedure involves a local volume averaging of the control volume (*cv*) based velocity field to the grid vertices and reverse averaging from the grid vertices to the *cv* centroids. The instantaneous DNS velocity field has been filtered so that $k_{\mathrm{filtered}} = 0.65 k_{\mathrm{DNS}}$.

Then, the particles have been tracked in a filtered (smoothed) velocity field. To determine the impact of smoothing on preferential concentration, the statistics of the particle number density in the physical space have been gathered. The pattern of preferential concentration is indeed modified by filtering. As noticed from the computed RDF of par-

ticle locations (Fig. 7b), the impact of the LES filtering is visible for the smaller-inertia particles ($St = 0.7$), correlated with the smaller eddy scales, and the resulting RDF in 3D becomes flatter for larger interparticle distance r. In the filtered velocity field, those particles behave as though their effective Stokes number were larger (the RDF for filtered $St = 0.7$ becomes close to that corresponding to DNS of $St = 2$ particles); yet, short-scale correlations remain strong. On the other hand, the RDF of $St = 2$ particles exhibits a steeper profile (up to $r \sim 10\eta_K$, say) upon filtering, indicating the lack of the small-scale fluid eddies that in the full DNS velocity field induce a stirring action. Therefore, the the shorter-range correlations become stronger in an *a priori* LES. This gives us some hint as to the construction of a SGS dispersion model. The snapshots of particle locations moving in the smoothed (LES-like) velocity field are shown in Figs. 8(b) and 9(b).

We have also checked the impact of filtering on the particle kinetic energy k_p(St). Results are shown in Table 1. As can be seen (DNS vs. *a priori* LES results without the SGS dispersion model), the turbulent kinetic energy is reduced in a filtered field (more for the smaller Stokes number studied). Then, we have considered the Lagrangian particle velocity autocorrelation. As observed in Fig. 10 (DNS vs. "no model LES" plots), because of the removal of smaller fluid eddies that basically induce a decorrelation of particle velocities ("random stirring"), the velocity correlation lasts longer. Consequently, the particle Lagrangian autocorrelation time scale T_p increases in *a priori* LES. As known from the theory of Tchen, the long-time particle dispersion coefficient is the product of k_p and T_p; consequently, the two effects partly compensate, so filtering is unlikely to have a major impact on the particle dispersion.

4. Reconstructing residual fluid velocity field along particle paths

4.1. *Reasons behind SGS dispersion modeling*

In LES, by definition of the method, a major part of the turbulent kinetic energy should be resolved (say, 80%, Pope 2000). Yet, this can be estimated only in simple cases where there is a DNS study at hand. For practically-relevant computations, the resolution often varies in space. The LES is known to face particular difficulties in wall-bounded flows, since the complete near-wall resolution becomes costly as the number of grid nodes scales roughly as $\mathrm{R}^{1.8}$ (cf. Pope 2000) and wall-modeling (or hybrid RANS/LES approach) is preferred. Also in this case, the SGS energy content may be considerable.

Regarding the LES of two-phase dispersed flows, several new issues appear. A concern about LES with the two-way coupling (of mass, momentum, energy) relates to the modeling of carrier phase source terms due to particles. Another concern, of importance here, is the impact of unresolved (subgrid-scale) flow quantities on particles: their dispersion, preferential concentration, deposition on walls. The effect can vary depending on the particle inertia parameter. In particular, for evaporating spray flow, the droplets become increasingly smaller and their inertia parameter changes, hence sooner or later the droplets unavoidably enter the size range where there is an impact from the flow SGS. In a numerical study of near-wall turbulence, Uijttewaal & Oliemans (1996) pointed out to the significant deviation of their LES results on particle deposition on the wall with respect to reference data. The LES predicted the particle deposition coefficient to be one order of magnitude smaller than the value found in experiment and DNS. A probable reason was the insufficient resolution of near-wall eddies responsible for deposition of smaller particles, and a need of a model to account for subgrid scale effects on particles was suggested.

4.2. *Requirements for a SGS particle dispersion model*

To specify criteria of a good SGS dispersion model, let us start from the well-established case of single-phase LES. Arguably, a sound model for the SGS stress should simulate the effects of small eddies without altering the motion at large-eddy scales. For particle-laden turbulent flows, but still with the one-way coupling of mass, momentum, and energy (i.e., no evaporation/condensation, light loading, no heat transfer), a pre-requisite for a good SGS dispersion model, suitable for FPT, is that particle characteristics should remain close to those from a fully-resolved computation. They include the statistics of instantaneous particle locations (preferential concentration, if any), averaged locations (e.g., the r.m.s. particle position in line-source dispersion, the concentration profile in jet or mixing layer), and velocities (turbulent kinetic energy, Lagrangian velocity autocorrelation).

The constraints to be satisfied by a SGS dispersion model are: (i) in the limit of fully-resolved computation (LES then becomes DNS, $k_{\rm sg} \to 0$), the model should have no effect on particle motion; (ii) in the limit of small particles ($\tau_p/\tau_f \to 0$ where τ_f is a characteristic fluid time scale) the model should boil down to the prediction of fluid diffusion; the velocity filtered density function (FDF) approach of Gicquel *et al.* (2002) may possibly serve as the limit case to compare with; (iii) in the limit of large particles ($\tau_p/\tau_f \to \infty$) the model should have no short-time effect on particle motion; (iv) in the presence of external force field (gravity), the model should possibly take it into account; (v) in the limit of under-resolved velocity field (LES then becomes RANS, $k_{\rm sg} \to k$), the particle turbulent dispersion should be fully modeled; (vi) for pairs of neighboring particles (located within the same cell or closer to each other than $\mathcal{O}(\Delta_f)$), the model should possibly account for relative dispersion effects.

We perceive the constraints (i)–(iii) as really important for SGS dispersion models in the context of LES. The effects of external fields (iv) are, apparently, not well known; the limit of RANS (v) is unlikely to be approached in real-life LES computations; finally, the relative dispersion (vi) cannot be accounted for in the one-point approach that is of interest here because of computational efficiency.

An essential ingredient of the SGS dispersion model is the residual kinetic energy $k_{\rm sg}$. It determines the level of residual velocity fluctuations, also those "seen" by particles. In a particular test case considered here (forced isotropic turbulence), $k_{\rm sg}$ can readily be found from the DNS data (raw and filtered). In general case, the subgrid kinetic energy of the flow can be estimated from its transport equation. Wang & Squires (1996) and Sankaran & Menon (2002) recall the $k_{\rm sg}$ equation based on the Schumann non-equilibrium model.

Alternatively, approximate expressions for the subgrid eddy viscosity ν_t can be explored and compared. Assuming that the cut-off wavenumber $k_c = 1/\Delta_f$ lies in the inertial range, the spectral analysis (cf. Lesieur, 1997) predicts $\nu_t = 0.267\sqrt{E(k_c)/k_c}$. Together with the assumption of the Pao energy spectrum, this yields $\nu_t = 0.067\Delta_f\sqrt{k_{sg}}$ where the proportionality constant has been given by Sankaran & Menon (2002); hence $k_{sg} = (\nu_t/0.067\Delta_f)^2$. Now, the eddy viscosity can be substituted from the SGS model used in actual LES computation.

4.3. *SGS dispersion model for locally homogeneous and isotropic turbulence*

A reasonable assumption about LES is to consider the residual turbulent motion as locally homogeneous and isotropic. Then, the fluid velocity "seen" by particles is computed as $U_i^* = \tilde{U}_i(\mathbf{x}_p, t) + u_i^*$, i.e. the sum of the filtered LES velocity $\tilde{U}_i$ interpolated at the particle location and the residual velocity "seen" by the particle. The assumption of the residual field being uncorrelated with the resolved one is implied here. It is quite strong for the

LES (yet correct in the RANS context) and can be partly justified by the fact that the model for u_i^*, proposed below, is meant to reconstruct some statistical quantities only (the energy and the time scale of the SGS fluid "seen"). An attempt to use the correlation of unresolved scales (just below the filter level) with the resolved ones (just above that level) is made in the approximate deconvolution models.

Crucial ingredients of a model to be put forward below refer to the residual fluid motion "seen" by the particle. They are the subgrid velocity scale of the fluid "seen", $\sigma_{\rm sg}^*$, and a subgrid time scale of the fluid "seen", τ_L^*. We assume in the following that the velocity scale of the fluid "seen" is equal to the characteristic SGS fluid velocity, $\sigma_{\rm sg}^* = \sigma_{\rm sg}$, where:

$$\sigma_{\rm sg} = \sqrt{\frac{2}{3} k_{\rm sg}} \; ; \tag{4.1}$$

yet, some error can occur due to preferential particle concentration. The timescale τ_L^* is generally a function of the SGS fluid time scale $\tau_{\rm sg}$, the time scale related to external fields, and possibly also of the particle relaxation time: $\tau_L^* = f(\tau_{\rm sg}, \sigma_{\rm sg}/g, \tau_p)$.

Langevin stochastic equation has been used in turbulent diffusion models on the one hand, and adopted in the Lagrangian PDF approach to turbulent flows in seminal developments by Pope and coworkers (cf. Pope 2000) on the other hand. From these two areas of application, the Langevin-type equations migrated to the modeling of two-phase dispersed flows. By analogy to modeling particle dispersion in isotropic turbulence in the context of statistical (RANS) description (Pozorski & Minier 1999), we assume that the SGS velocity "seen" $\mathbf{u}^*$ is governed by the Langevin equation

$$du_i^* = -\frac{u_i^*}{\tau_L^*}\, dt + \sqrt{\frac{2\sigma_{\rm sg}^2}{\tau_L^*}}\, dW_i \tag{4.2}$$

where dW_i is an increment of the Wiener process (Gardiner 1990). We note that in LES (and in non-homogeneous RANS) the equation for the SGS (or turbulent) fluid velocity contains two more RHS terms: the gradient of the SGS (or turbulent) stress, $(\partial \tau_{ij}/\partial x_j)dt$, and the filtered (or mean) velocity gradient term, $-u_j^*(\partial \tilde{U}_i/\partial x_j)dt$; cf. Pope (2000) and Minier & Peirano (2001, Sec. 6.7.2) for RANS and Fede *et al.* (2006) for LES. Such a Langevin-type equation (with the two "turbophoretic" terms present) for residual fluid motion should always be used in more complex turbulent flows simulated with LES (spurious drifts will appear otherwise). We argue that in isotropic turbulence, there is no significant "turbophoretic" effect due to filtered velocity gradients (which are smooth) inducing any mean drift, and the gradients of the SGS stress tensor are correlated over a short length scale ($\sim \Delta_f$) only. This provides us with a partial justification of the neglect of these terms in a homogeneous isotropic turbulence considered in the paper.

In Eq. (4.2), the time scales of residual motions "seen" by the particle are related to $\tau_{\rm sg}$ (the time scale of residual fluid motions), estimated from:

$$\tau_{\rm sg} = C \frac{\Delta_f}{\sqrt{\frac{2}{3} k_{\rm sg}}} \; . \tag{4.3}$$

The model constant $C = \mathcal{O}(1)$ accounts for the uncertainty concerning the time scale of the residual velocity autocorrelation. The prediction $\tau_L^* = \tau_{\rm sg}$ is expected to work well for small St (also in the limit case of fluid diffusion). For larger St, we tentatively propose an extension of the model for RANS particle dispersion (Pozorski & Minier 1999) drawing on the Csanady expressions to account for the crossing-trajectory effect. The time scale

will now differ in the directions parallel and perpendicular to the relative velocity $\tilde{\mathbf{U}}-\mathbf{U}_p$

$$\tau^*_{L,||} = \frac{\tau_{\rm sg}}{\sqrt{1+\beta^2\xi^2}}\,, \quad \tau^*_{L,\perp} = \frac{\tau_{\rm sg}}{\sqrt{1+4\beta^2\xi^2}} \tag{4.4}$$

where ξ is the normalized drift velocity determined from $\xi = |\tilde{\mathbf{U}} - \mathbf{U}_p|/\sigma_{\rm sg}$. Note that the relative velocity in RANS is computed from the mean values as $|\langle\mathbf{U}\rangle - \langle\mathbf{U_p}\rangle|$; yet, in LES the filtered particle velocity is not available (by definition, spatial smoothing can only be applied to field variables). Therefore, we decided to keep $\mathbf{U}_p$ in the expression. In the context of RANS, β in Eqs. (4.4) represents the ratio of Lagrangian to Eulerian time scales $\beta = T_L/T_E$; here, we assume $\beta = 1$ for SGS velocity field. Also note that, unlike stochastic models proposed by Shotorban & Mashayek (2006) and Fede *et al.* (2006), the statistics of the SGS fluid "seen" used to close the Langevin equation are different from those of the SGS fluid motion. To sum up: the present choice of choice of τ^*_L means that the SGS fluid velocity "seen" is autocorrelated over the time scale of the residual motion, being of the order of Δ_f/u_{sg} for the smallest particles (that behave like fluid ones) or correspondingly shorter for particles of larger inertia, taking into account the crossing-trajectory effect, Eq. (4.4).

In practical implementation, a discrete version of the model (unconditionally stable, first-order accuracy in time) becomes

$$u_i^{*(n+1)} = a u_i^{*(n)} + b\xi_i \tag{4.5}$$

where $\Delta t = t^{(n+1)}$–$t^{(n)}$ is the time interval and ξ_i are random numbers from the standard Gaussian distribution, $\xi_i \in \mathcal{N}(0,1)$. The values of a and b are given by the explicit solution of the stochastic differential equation (SDE), Eq. (4.2), with frozen coefficients over a time step Δt:

$$a = e^{-\Delta t/\tau^*_L}\,, \qquad b = \sigma_{\rm sg}\sqrt{1-e^{-2\Delta t/\tau^*_L}}\,. \tag{4.6}$$

In the particular example of Eq. (4.2), which is a SDE with constant coefficients, the solution provided by Eqs. (4.5) and (4.6) is exact. Higher-order numerical schemes for this class of SDEs have recently been proposed (Peirano *et al.* 2006). However, the construction of higher-order schemes for general (variable coefficients) SDEs (Kloeden & Platen 1992) remains an open issue.

Equation (4.5) can be further simplified to the Euler scheme

$$u_i^{*(n+1)} = \left(1-\frac{\Delta t}{\tau^*_L}\right) u_i^{*(n)} + \sigma_{\rm sg}\sqrt{\frac{2\Delta t}{\tau^*_L}}\,\xi_i\,. \tag{4.7}$$

Yet, in contrast to formulation (4.5)–(4.6), discretization (4.7) does impose a time step restriction $\Delta t < \tau^*_L$ because of stability concerns.

It may be interesting to note that in the limit of $\Delta t \gg \tau^*_L$ the scheme (4.5) boils down to generating a series of independent successive velocities $\mathbf{u}^*$, i.e.

$$\mathbf{u}^{*(n+1)} = \sigma_{\rm sg}\boldsymbol{\xi}\,. \tag{4.8}$$

However, for a physically-consistent use of Eq. (4.8), it is imperative that the time intervals for generating a series of independent velocity realizations be $2\tau^*_L$ in order to preserve the correlation time scale (cf. Pozorski & Minier 1998). These time intervals should not be related to the time step of fluid simulations, although this aspect is sometimes overlooked in papers applying random-walk type models for SGS particle dispersion in LES.

[NB: In our case, this behavior is implied by the choice of the model constant $C = 0$ in a discrete setting, cf. Eqs. (4.3) and (4.6).]

5. Results of the SGS dispersion model

5.1. *Particle velocity statistics*

We start here with the particle statistics that are classical mean quantities (widely-used also in RANS); in the next section, we will discuss statistics of particle locations, and specially their segregation in space, which are two-point statistics (more subtle, say), specific to LES rather than RANS. We note that the segregation, although formally quantified through two-point correlations (the statistics of interparticle distance), results from the (one-point) correlations of fluid and particle velocities.

We have computed the particle turbulent kinetic energy from FPT with the SGS dispersion model (4.2) in *a priori* LES computations of forced isotropic turbulence for the same conditions as those described in Sec. 3.3. Because the maximum of preferential concentration in DNS is achieved around $St = 1$, for further studies we have chosen a slightly smaller ($St = 0.7$) and slightly larger value ($St = 2$) of particle inertia, since we suppose that the impact of filtering and a subsequent effect of the SGS dispersion model will be qualitatively different for particle inertia located on the opposite sides of the maximum.

Results are shown in Table 1. As readily noticed, the particle kinetic energy increases with increasing model constant C. The DNS energy level can be restored in the simulations for a suitable choice of the model constant; for the Stokes numbers studied, $C = 1$ works quite well as far as the turbulent energy of particles is concerned.

The particle velocity autocorrelations are plotted in Fig. 10. As discussed before, the filtering ("no model" LES results) tends to increase the correlation for intermediate time intervals. The effect of the Langevin-type SGS particle dispersion model, by its very nature, is to add some random decorrelation, the stronger the larger is the model constant C. The conclusion here is that the Langevin-type SGS dispersion model can not be tuned to satisfy the two constraints: a correct level of particle kinetic energy on the one hand, and a correct Lagrangian velocity correlation and the preferential concentration patterns on the other hand. Recently, an interesting proposal of separating the particle velocity in turbulent flow into a continuous field and a random (uncorrelated) part has been put forward by Février *et al.* (2005). Arguably, LES filtering affects both, and the Langevin-type, stochastic diffusion model is suitable as a remedy to the effect of filtering on the uncorrelated part only.

5.2. *Preferential concentration*

Next, we have found the statistics of the instantaneous particle locations resulting from *a priori* LES. The computational results for two values of the Stokes number and some choices of the model constant are shown in Figs. 8 and 9. The impact of the residual velocity field, reconstructed in FPT, is readily noticed. As expected, the one-point stochastic model introduced here has a "randomizing" effect on particle locations. For particle sizes larger than that of maximum preferential concentration effect (roughly $\mathrm{St} \approx 1$ in our case) the randomizing effect of small scales is lost (the picture of preferential concentration becomes overly sharp), so the model is meant to restore it, cf. Fig. 9. In the case of smaller particles that are most influenced by smaller eddies and correlated on a shorter length scale, it is shown in Fig. 8 that the filtering does an inverse effect, i.e. it partly kills

this short-scale preferential concentration (the picture of preferential concentration becomes somewhat "blurred"), so a potentially successful model for this case should rather be of an "antidiffusive" character (arguably, scale-similarity arguments can be used for its construction). As found from the instantaneous particle snapshots (Figs. 8 and 9), the choice of the model constant to restore the turbulent energy of particles, $C \approx 1$ is not suitable as far as the preferential concentration patterns are concerned since already $C = 0.1$ tends to destroy them.

To confirm the visual evidence of Figs. 8 and 9, we have computed again some measures of preferential concentration (cf. Sec. 3.2). Now, also to enhance the visibility of changes due to filtering and subsequent modeling, the RDF is computed with particles located in 2D cuts (slices, about 2% thick) of the computational box. Figure 11 shows the impact of the SGS dispersion model on the statistics of preferential concentration, as quantified by the RDF and compared to Fig. 7(b). The observation for smaller inertia particles ($St = 0.7$) is that even the *a priori* LES results (no model) show a slightly flatter RDF (less structure) than the DNS case. Consequently, application of the stochastic diffusion model further decreases the preferential concentration. On the other hand, for larger inertia particles ($St = 2$) the *a priori* LES with no model shows a steeper RDF profile than the DNS, meaning that the preferential concentration becomes more pronounced for this combination of particle inertia and the filter size. Conclusion here is that the SGS model does a better job for $St = 2$ where some random stirring of particles due to the smaller fluid scales (removed by LES filtering) is restored by the stochastic diffusion model of the Langevin type, Eq. (4.2). However, the model is not able to retrieve the DNS preferential concentration patterns for particles of $St = 0.7$ (and smaller).

6. Conclusion and future plans

In the present paper, we have investigated the impact of filtered velocity field, typically used in LES, on particle motion in two-phase turbulent flows. In particular, the changes in particle preferential concentration patterns have been quantified. Then, a stochastic model has been proposed to reconstruct the residual velocity field along heavy particle trajectories, accounting for the crossing-trajectory effect. The model is able to retrieve a correct level of particle turbulent kinetic energy. For smaller-inertia particles that are preferentially-concentrated with the flow scales filtered out by the LES, a diffusion-type SGS dispersion model proposed in the paper is not able to retrieve the small-scale patterns of particle segregation. For larger-inertia particles, small scales filtered out in LES have a randomizing effect on particle spatial distribution and this effect is well simulated by our SGS dispersion model. It can thus be recommended for use in situations involving larger-inertia particles that are still susceptible to filtering. For smaller-inertia particles, the model is still helpful in restoring correctly the short-time dispersion and the particle turbulent kinetic energy.

A lingering question as to the present SGS particle dispersion model is that it is only a single-realization (one-particle) approach. The statistical interpretation of the model has to be thought over, including the inhomogeneous turbulence, and also in the context of parcels (representing many solid particles). Possibly, along more general ideas of stochastic modeling (beyond the Langevin equation), an improved model should consist of a random ingredient (since the details of residual fluid motion are unknown) and possibly also of a deterministic ingredient, dependent on the structure of the resolved

field and justified by the hope that the largest unresolved scales are in a sense similar to resolved ones.

The stochastic Langevin model proposed for SGS particle dispersion is one-point by construction. Hence, it is able to correctly reconstruct the particle turbulent kinetic energy and the long-time dispersion. Otherwise, to exactly account for two-particle quantities (such as relative dispersion, relative velocity statistics, or SGS preferential concentration effects), a structural approach, trying to mimic most important features of the subgrid-scale flow field, should be conceived.

A further-term objective is to unify the LES/FPT approach for the dispersed flows, presented above, with the LES/FDF approach for flows with scalars, possibly reactive, developed by Colucci *et al.* (1998). This should ultimately provide a physically-sound, yet efficient, tool for the computation of dispersed turbulent two-phase flows with chemical reactions (spray combustion).

Acknowledgments

Part of this work was completed during the 2004 Summer Program held at Stanford University, Center for Turbulence Research (CTR). We are grateful to Professor John Eaton for his comments on an earlier version of the paper that appeared in the proceedings of the CTR Summer Program. Insightful remarks and suggestions of an unknown Referee #3 are very much appreciated. Our sincere thanks also extend to Venkat Raman (now at University of Texas, Austin) and Jean-Pierre Minier (R&D Division, Electricité de France) for stimulating discussions.

REFERENCES

Apte, S. V., Mahesh, K., Moin, P. & Oefelein, J. C. 2003a LES of swirling particle-laden flows in a coaxial-jet combustor. *Int. J. Multiphase Flow* **29**, 1311–1331.

Apte, S. V., Gorokhovski, M. & Moin, P. 2003b LES of atomizing spray with stochastic modeling of secondary breakup *Int. J. Multiphase Flow* 29, 1503–1522.

Armenio, V., Piomelli, U. & Fiorotto, V. 1999 Effect of the subgrid scales on particle motion. *Phys. Fluids* **11**, 3030–3042.

Bagchi, P. & Balachandar, S. 2003 Effect of turbulence on the drag and lift of a particle. *Phys. Fluids* **15**, 3496–3513.

Boivin, M., Simonin, O. & Squires, K. D. 2000 On the prediction of gas-solid flows with two-way coupling using large eddy simulation. *Phys. Fluids* **12**, 2080–2090.

Burton, T. M. & Eaton, J. K. 2003 Fully resolved simulations of particle-turbulence interaction. *Rep. No. TSD–151*, Dept. of Mech. Engng., Stanford University.

Colucci, P. J., Jaberi, F. A., Givi, P. & Pope, S. B. 1998 Filtered density function for large eddy simulation of turbulent reacting flows. *Phys. Fluids* **10**, 499–515.

Eaton, J. & Fessler, J. R. 1994 Preferential concentration of particles by turbulence. *Int. J. Multiphase Flow* **20**, Suppl., 169–209.

Fede, P. & Simonin, O. 2006 Numerical study of the subgrid turbulence effects on the statistics of heavy colliding particles. *Phys. Fluids* **17**, 045103.

Fede, P., Simonin, O., Villedieu, P. & Squires, K. D. 2006 Stochastic modelling of the turbulent subgrid fluid velocity along inertial particle trajectories. *Proceedings of the Summer Program*, Center for Turbulence Research, Stanford University, pp. 247-258.

Février, P., Simonin, O. & Squires, K. D. 2005 Partitioning of particle velocities in gas-solid turbulent flows into a continuous field and a spatially uncorrelated random distribution: theoretical formalism and numerical study. *J. Fluid Mech.* **533**, 1–46.

Fox, R. O. 2003 *Computational Models for Turbulent Reacting Flows.* Cambridge University Press.

Gardiner, C. W. 1990 *Handbook of Stochastic Methods for Physics, Chemistry and the Natural Sciences*, corrected 2nd ed. Springer-Verlag, Berlin.

Gicquel, L. Y. M., Givi, P., Jaberi, F. A. & Pope, S. B. 2002 Velocity filtered density function for LES of turbulent flows. *Phys. Fluids* **14**, 1196–1213.

Hogan, R. C. & Cuzzi, J. N. 2001 Stokes and Reynolds number dependence on preferential particle concentration in simulated 3D turbulence. *Phys. Fluids* **13**, 2938–2945.

Kuerten J. G. M. 2006 Subgrid modeling in particle-laden channel flow. *Phys. Fluids* **18**, 025108.

Kuerten J. G. M. & Vreman A. W. 2005 Can turbophoresis be predicted by large-eddy simulation? *Phys. Fluids* **17**, 011701.

Lesieur M. (1997) *Turbulence in Fluids*, 3rd enlarged edition. Kluwer, Dordrecht.

Lundgren, T. S. 2003 Linearly forced isotropic turbulence, *Annual Research Briefs*, Center for Turbulence Research, 461–473.

MacInnes, J. M. & Bracco, F. V. 1992 Stochastic particle dispersion modeling and the tracer-particle limit. *Phys. Fluids A* **4**, 2809–2824.

Mashayek, F. & Pandya, R. V. R. 2003 Analytical description of two-phase turbulent flows. *Prog. Energy Combust. Sci.* **29**, 329–378.

Maxey, M. R. 1987 The motion of small spherical particles in a cellular flow field. *Phys. Fluids* **30**, 1915–1928.

Maxey, M. R. & Riley, J. J. 1983 Equation of motion for a small rigid sphere in a nonuniform flow. *Phys. Fluids* **26**, 883–889.

Miller, R. S. & Bellan, J. 2000 Direct numerical simulation and subgrid analysis of a transitional droplet laden mixing layer. *Phys. Fluids* **12**, 650–671.

Minier, J. P. & Peirano, E. 2001 The PDF approach to turbulent polydispersed two-phase flows. *Phys. Reports* **352**, 1–214.

Minier, J. P., Peirano, E. & Chibbaro, S. 2004 PDF model based on Langevin equation for polydispersed two-phase flows applied to a bluff-body gas-solid flow. *Phys. Fluids* **16**, 2419–2431.

Minier, J. P. & Pozorski, J. 1997 Relations between the Kinetic Equation model and the Langevin Equation model in two-phase flow modelling. *ASME Fluids Engineering Division Summer Meeting*, Vancouver, Canada, 22-26 June, ASME FEDSM 97-3616.

Moin, P, & Apte, S.V. 2006 LES of multiphase reacting flows in complex combustors. *AIAA J.* **44**, 698–708.

Okong'o, N. & Bellan, J. 2000 *A priori* subgrid analysis of temporal mixing layers with evaporating droplets. *Phys. Fluids* **12**, 1573–1591.

Okong'o, N. A. & Bellan, J. 2004 Consistent large-eddy simulation of a temporal mixing layer laden with evaporating drops. Part 1. Direct numerical simulation, formulation and *a priori* analysis. *J. Fluid Mech.* **499**, 1–47.

Peirano, E., Chibbaro, S., Pozorski, J. & Minier, J. P. (2006) Mean-field/PDF numerical approach for polydispersed turbulent two-phase flows. *Prog. Energy Combust. Sci.* **32**, 315–371.

Pope, S. B. 2000 *Turbulent Flows.* Cambridge University Press.

Pozorski, J. 1998 A derivation of the kinetic equation for dispersed particles in turbulent flows. *J. Appl. Theor. Mech.* **36**, 31–46.

Pozorski, J. & Minier, J. P. 1998 On the Lagrangian turbulent dispersion models based on the Langevin equation. *Int. J. Multiphase Flow* **24**, 913–945.

Pozorski, J. & Minier, J. P. 1999 PDF modeling of dispersed two-phase turbulent flows. *Phys. Rev. E* **59**, 855–863.

Reade, W. C. & Collins, L. R. 2000 Effect of preferential concentration on turbulent collision rates. *Phys. Fluids* **12**, 2530–2540.

Reeks, M. W. 1992 On the continuum equations for dispersed particles in nonuniform flows. *Phys. Fluids A* **4**, 1290–1303.

Sankaran, V. & Menon, S. 2002 LES of spray combustion in swirling flows. *J. Turbulence* **3**, art. no. 011.

Sawford, B. L. 2001 Turbulent relative dispersion. *Annu. Rev. Fluid Mech.* **33**, 289–317.

Segura, J. C., Eaton, J. K. & Oefelein, J. C. 2004 Predictive capabilities of particle-laden LES. *Rep. No. TSD–156*, Dept. of Mech. Engng., Stanford University.

Shotorban, B. & Mashayek, F. 2005 Modeling subgrid-scale effects on particles by approximate deconvolution. *Phys. Fluids* **17**, 081701.

Shotorban, B. & Mashayek, F. 2006 A stochastic model of particle motion in large-eddy simulation. *J. Turbulence* **7**, art. 18.

Simonin, O. 1996 Eulerian numerical approach for prediction of of gas-solid turbulent two-phase flows. *Von Karman Institute Lecture Series*, Rhode-St-Genèse, Belgium.

Squires, K. D. & Eaton, J. K. 1991 Preferential concentration of particles by turbulence. *Phys. Fluids A* **3**, 1169–1178.

Stock, D. E. 1996 Particle dispersion in flowing gases. *J. Fluids Engng.* **118**, 4–17.

Thomson, D.J. 1986 Criteria for the selection of stochastic models of particle trajectories in turbulent flows. *J. Fluid Mech.* **180**, 529–556.

Uijttewaal, W. S. J. & Oliemans, R. V. A. 1996 Particle dispersion and deposition in DNS and LES of vertical pipe flows. *Phys. Fluids* **8**, 2590–2604.

Wang, L. P. & Maxey, M. R. 1993 Settling velocity and concentration distribution of heavy particles in homogeneous isotropic turbulence. *J. Fluid Mech.* **256**, 27–68.

Wang, Q. & Squires, K. D. 1996 Large eddy simulation of particle-laden turbulent channel flow. *Phys. Fluids* **8**, 1207–1223.

Zaichik, L. I. & Alipchenkov, V. M. 2003 Pair dispersion and preferential concentration of particles in isotropic turbulence. *Phys. Fluids* **15**, 1776–1787.

	DNS	*a priori* LES	model, $C = 0.1$	model, $C = 1$
St $= 0.7$	0.83	0.54	0.60	0.77
St $= 2$	0.60	0.42	0.46	0.62

TABLE 1. Turbulent kinetic energy of particles normalised with the fluid energy ("model": *a priori LES* with the SGS dispersion model).

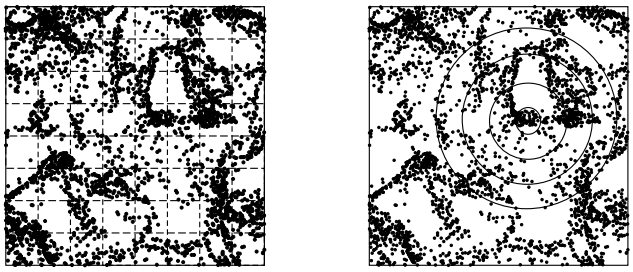

FIGURE 1. Computing the particle number density and the radial distribution function.

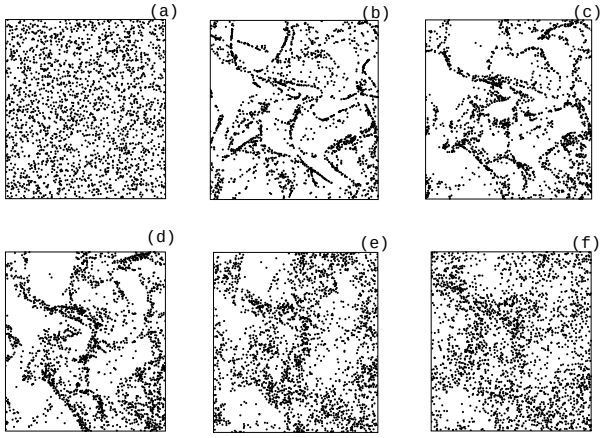

FIGURE 2. Snapshots of particle positions from DNS; runs with various values of the particle inertia parameter: a) St $= 0.01$, b) St $= 0.2$, c) St $= 0.7$, d) St $= 1$, e) St $= 2$, f) St $= 4$.

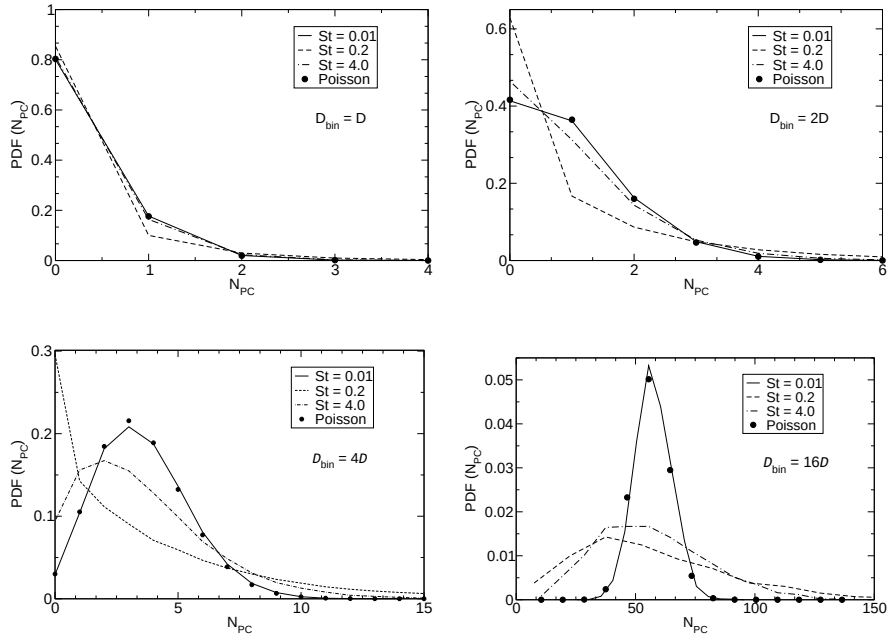

FIGURE 3. PDF of particle number density for different bin sizes: a) Δ_f, b) $2\Delta_f$, c) $4\Delta_f$, d) $16\Delta_f$.

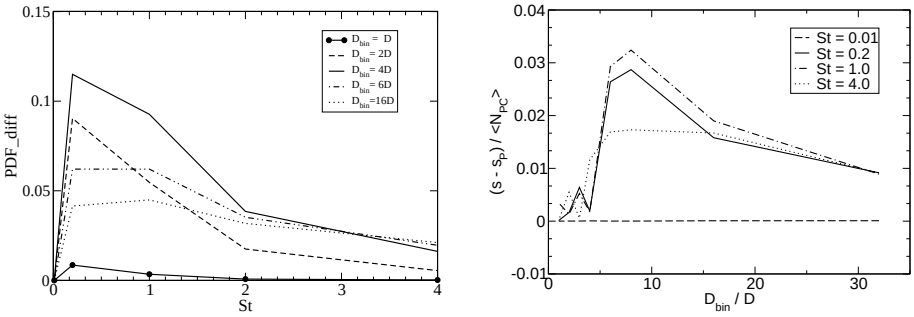

FIGURE 4. Measures of preferential concentration: a) difference of PDFs of particle number density (actual and Poisson), Eq. (3.2); b) difference of standard deviations, Eq. (3.3).

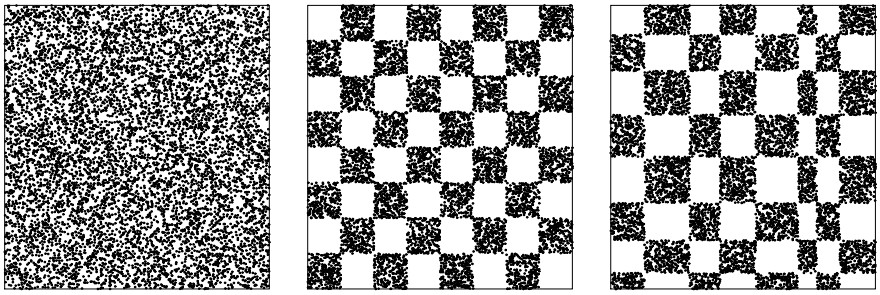

FIGURE 5. Various particle arrangements for RDF testing: a) uniform, b) regular checkered, c) randomized checkered.

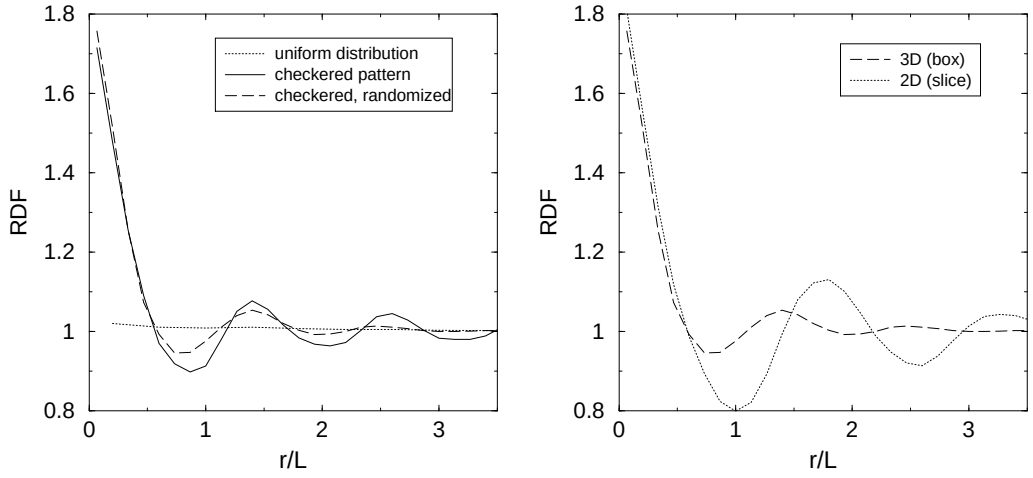

FIGURE 6. Particle radial distribution functions: a) for all pre-arranged patterns in 3D, b) for the checkered, randomized pattern in 2D and 3D.

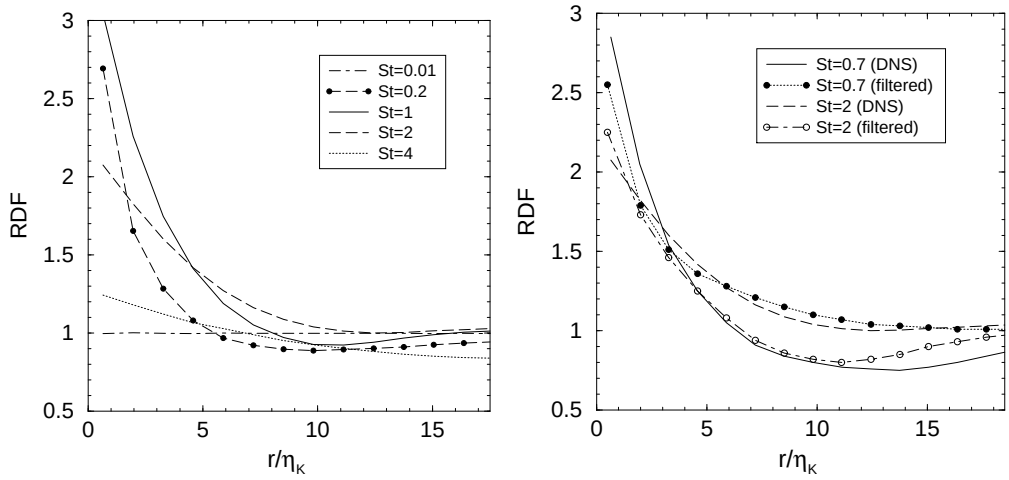

FIGURE 7. Radial distribution function of heavy particle locations. Fluid velocity computed in: (a) DNS for all St; (b) DNS and *a priori LES* (filtered) for $St = 0.7$ and $St = 2.0$.

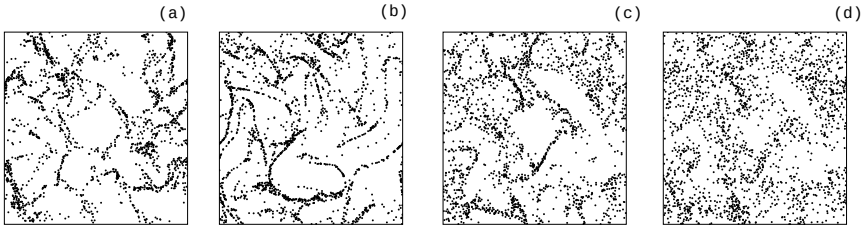

FIGURE 8. Snapshots of particle positions; runs for particles of St = 0.7. a) DNS; b) *a priori* LES with with no FPT model; c) *a priori* LES with FPT model and C=0; d) with C=0.05.

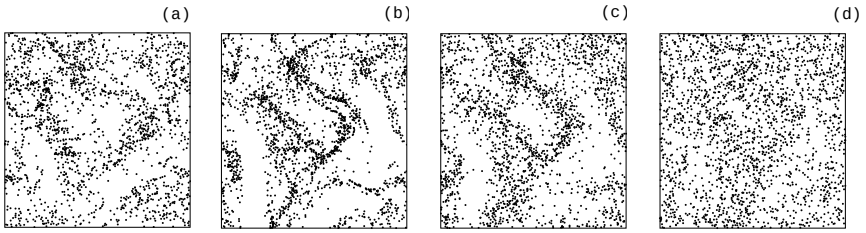

FIGURE 9. Snapshots of particle positions; runs for particles of St = 2. a) DNS; b) *a priori* LES with no FPT model; c) *a priori* LES with FPT model and C=0.05; d) with C=1.

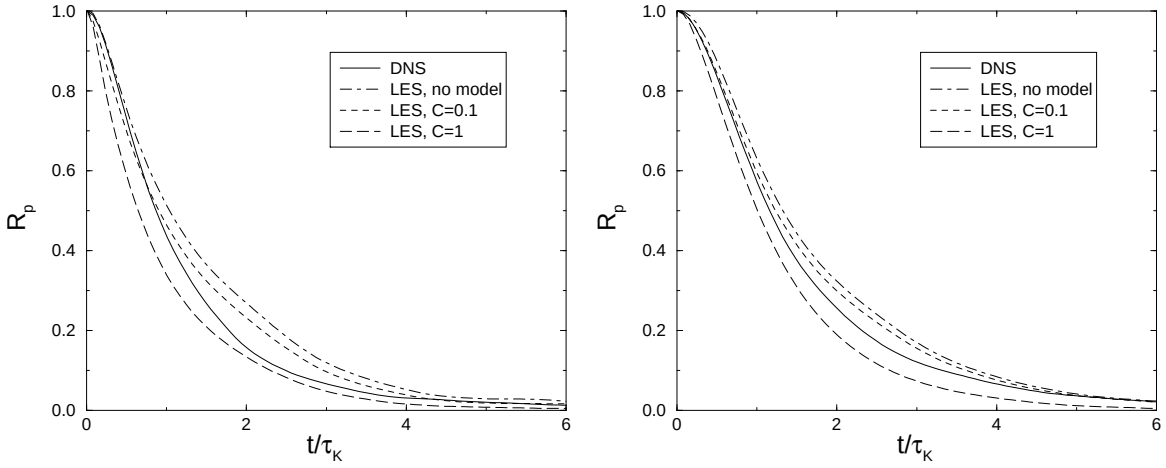

FIGURE 10. Particle velocity autocorrelation function: a) St = 0.7; b) St = 2.

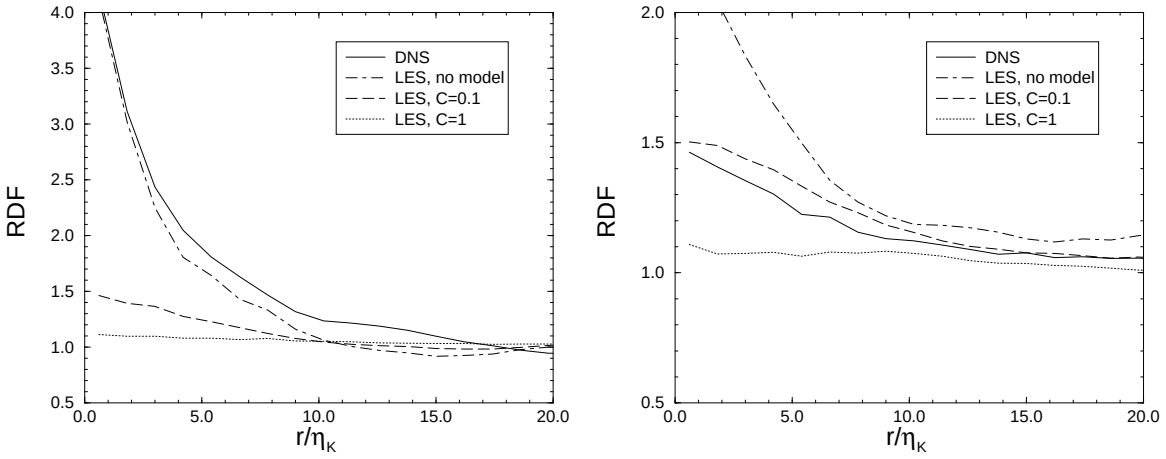

FIGURE 11. RDF of particles: a) St = 0.7; b) St = 2. Results for DNS, *a priori* LES with no SGS dispersion model, and LES with the model of Eq. (4.2); two different choices of the model constant, Eq. (4.3).